



ELSEVIER

Contents lists available at SciVerse ScienceDirect

Nuclear Instruments and Methods in Physics Research A

journal homepage: www.elsevier.com/locate/nima

Neutron detection in a high gamma-ray background with EJ-301 and EJ-309 liquid scintillators

L. Stevanato^{a,*}, D. Cester^a, G. Nebbia^b, G. Viesti^a^a Dipartimento di Fisica ed Astronomia dell' Università di Padova, Fisica "Galileo Galilei", Via Marzolo 8, I-35131 Padova, Italy^b INFN Sezione di Padova, Via Marzolo 8, I-35131 Padova, Italy

ARTICLE INFO

Article history:

Received 20 April 2012

Received in revised form

1 June 2012

Accepted 19 June 2012

Available online 4 July 2012

Keywords:

Liquid scintillator

Digital signal processing

ABSTRACT

Using a fast digitizer, the neutron–gamma discrimination capability of the new liquid scintillator EJ-309 is compared with that obtained using standard EJ-301. Moreover the capability of both the scintillation detectors to identify a weak neutron source in a high gamma-ray background is demonstrated. The probability of neutron detection is $PD=95\%$ at 95% confidence level for a gamma-ray background corresponding to a dose rate of 100 $\mu\text{Sv/h}$.

© 2012 Elsevier B.V. All rights reserved.

1. Introduction

Organic liquid scintillators are commonly employed for fast neutron detection thanks to their pulse shape discrimination (PSD) capability used to separate neutrons from the gamma-ray component of the radiation field (see for example [1]). Being the liquid scintillator a standard tool in basic research [2], such detectors have found a rather marginal use in Homeland Security applications since many operational contexts prohibit these liquids because of their toxicity and flammability. Moreover liquid scintillators detect neutron above a low energy threshold (usually few hundred keV) and exhibit a good gamma-ray efficiency so that such detectors are normally characterized by a modest gamma-ray rejection capability, a property that is required to identify weak neutron source in a strong gamma-ray background [3].

However, it has been recently pointed out that selecting the fast neutron energy region in the total neutron spectrum optimizes the signal-to-background ratio thus improving the detection of weak neutron sources [4]. New liquid scintillation materials have become recently available as the EJ-309 type [5], from Eljen Technology, which is characterized by low toxicity and high flash point (144 °C) compared to the more traditional EJ-301 (flash point 26 °C) which is equivalent to the well known NE-213.

The EJ-309 scintillator has been employed in pure and applied research works confirming a PSD capability well suited to perform

neutron spectroscopy [6,7]. Moreover the gamma rejection capability of the EJ-309 was the subject of a recent study [8].

In this work we will study the possible application of liquid scintillator detectors in the field of Homeland Security with respect to neutron detection in an intense gamma-ray background.

2. Experimental details

The detectors studied in this work consist of 2 in. \times 2 in. liquid scintillator cells coupled to an H1949-51 HAMAMATSU photomultiplier (PMT) through an EJ-560 silicon rubber interface.

The PMT anode signals were directly fed into a CAEN V1720 12 bit 250 MS/s Digitizer. The PMTs are operated at relatively low voltage ($HV=1600\text{ V}$), to avoid saturation effects in digitizing the pulses. Inside the V1720 card, Digital Pulse Processing (DPP) algorithms are implemented using FPGA, providing on-line for each event (a) a time stamp, (b) a complete integration of the signal, (c) a partial integration of the signal used for PSD and (d) the possibility of storing a selected part of the digitized signal. Consequently, in the V1720 card some parameters need to be tuned in order to optimize the PSD, once the “Long Gate” (i.e. the number of FADC bins used in the total pulse integration) is properly set. Such parameters are the “Short Gate” (i.e. the number of FADC bins used in the integration of the fast part of the pulse), the “Pre-Gate” (establishing the point before the crossing of the low energy threshold from which the integration is started) and the “Baseline Threshold” (i.e. the number of points used for the definition of the baseline level). In our experimental set-up the PSD parameter is then computed on-line as

* Corresponding author. Tel.: +39 0498275936.

E-mail address: luca.stevanato@pd.infn.it (L. Stevanato).

$PSD = (\text{Long Gate Integration} - \text{Short Gate Integration}) / \text{Long Gate Integration}$.

In order to characterize the neutron–gamma discrimination capability we used the Figure of Merit (FoM) obtained by analyzing the PSD distribution from a ^{252}Cf source. It is defined as $FoM = S / (\Gamma_e + \Gamma_p)$ where S is the difference between the two centroids of the neutron and gamma peaks and $(\Gamma_e + \Gamma_p)$ is the sum of the gamma and neutron full widths at half maximum [FWHM] [9]. The optimization of the DPP parameters has been performed empirically by maximizing the FoM corresponding to different sets of the DPP parameters. It is found that the optimized DPP parameters for the EJ-301 and EJ-309 detectors are identical: 70 and 17 bins for the Long and Short Gates, respectively, 10 bins for the Pre-gate and 4 bins for the Baseline Threshold (each bin is 4 ns wide). With the above parameters, each pulse is characterized by 70 samples and the V1720 Digitizers handles count rate up about 100 kHz without dead time.

Finally, the energy calibration of the scintillation light was established by using the procedure described in [10] based on the fit of the experimental pulse shape distribution by using the theoretical Compton scattering distribution with an empirical spreading width to account for the finite detector resolution. Samples of those spectra for a ^{22}Na radioactive source are reported in Fig. 1.

It is immediately evident from Fig. 1 that the spectra measured with the two scintillators are very similar. The calibration procedure allows one to obtain an estimate of the detector pulse height resolution by determining the spreading width σ needed

to reproduce the Compton Edge structures (for more details see [10]). The energy resolution is defined as σ/L where L is the energy value of the Compton Edge. The energy resolution derived in this case for the two liquid scintillators is $\sigma/L = 6.0\%$ for the Compton Edge of the 1275 keV gamma-ray ($\sigma/L = 8.2\%$ for the Compton Edge of the 511 keV gamma-ray). This figure is slightly better with respect to those reported in [10] for a 2 in. \times 2 in. EJ-228 plastic scintillator processed with standard NIM electronics.

Finally, the low energy detection threshold, as determined from the spectra in Fig. 1, results to be about 60 keV.

3. Pulse shape discrimination

The response of the different scintillators was studied using a weak ^{252}Cf source (0.7×10^4 neutron/s) placed at about 15 cm from the detector front face. Typical PSD versus energy scatter plots are shown in Fig. 2. In this representation the neutron and gamma regions can be separated by a cut at $PSD = 0.09$ for the EJ-301 and $PSD = 0.16$ for the EJ-309 for energies larger than 300 keV.

A number of PSD spectra have been produced by varying the low energy threshold and analyzed. Extracted FoM values are reported in Fig. 3 for the two detectors explored in this work as a function of the low energy threshold.

It is seen from Fig. 3 that the FoM increases, improving the discrimination, with the low energy threshold reaching values $FoM > 1.5$ for thresholds of about 300 keV. This threshold value corresponds to about 1.5 MeV in proton energy by using the

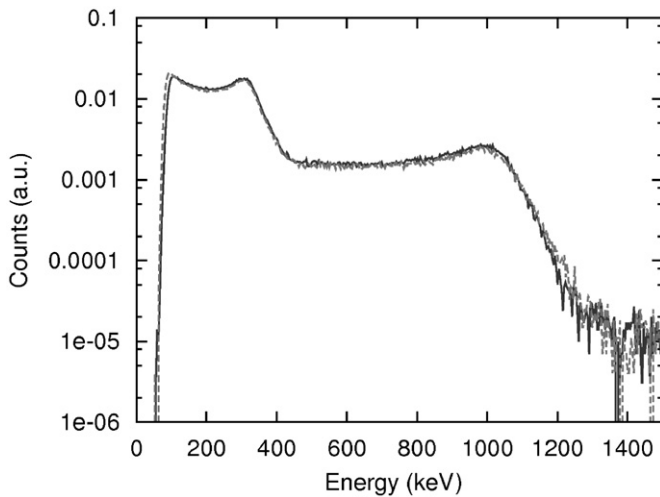


Fig. 1. Calibrated ^{22}Na pulse height distribution for the detectors studied in this work: EJ-301 full line, EJ-309 dashed line.

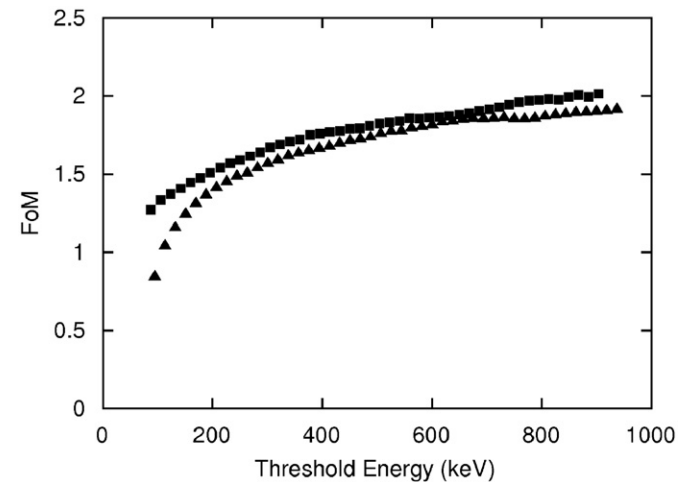


Fig. 3. Figure-of-Merit parameter (FoM) as a function of the low energy threshold for the detectors studied in this work. EJ-301 detected as squares and EJ-309 as triangles. The statistical uncertainties are within the point size.

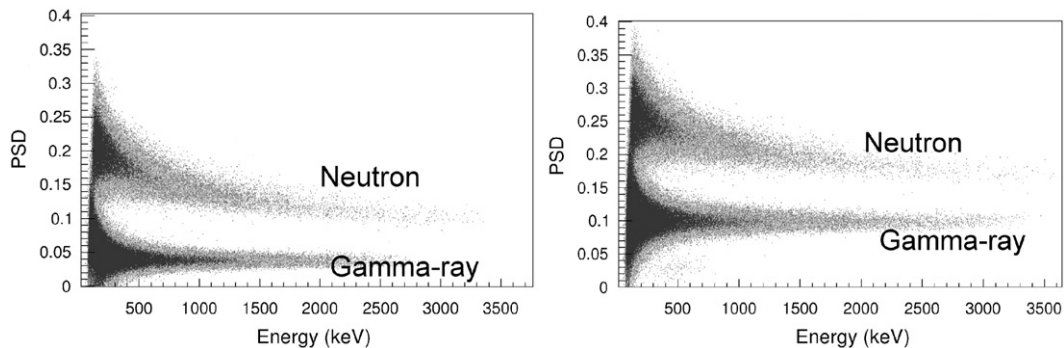


Fig. 2. Scatter plot PSD versus energy of a ^{252}Cf source measured with the EJ-301 detector (left) and EJ-309 (right).

response functions provided in [11]. The slightly lower pulse shape capability of the EJ-309 with respect to the EJ-301 is also confirmed, although the measured FoM values for the two detectors are fairly closed.

The FoM values measured for the EJ-301 in the present work can be compared with the $FoM=1.6–1.8$ for 4 in. \times 2 in. detectors employing the same liquid scintillator for a threshold of 1.5 MeV proton energy [11] and $FoM=1.61–1.68$ for a 2 in. \times 2 in. BC-501A scintillator for thresholds of 0.6 and 1.0 MeV proton energy, respectively [12].

4. Gamma-ray rejection capability

As discussed in detail in [13], it is required that the neutron detectors employed in Homeland Security applications shall be able to detect the presence of neutrons inside a high gamma-ray background. As an example, for hand-held instruments the relevant requirements are contained in the IEC62244 standard [14]. In this case, it is mandatory that the instrument generates a neutron alarm within 10 s sampling time when a 10 ng unmoderated ^{252}Cf source (equivalent to 2×10^4 neutron/s) is placed at 25 cm from the detector, which is equivalent to a distance of 15 cm for our 0.7×10^4 neutron/s source.

At the same time it is generally required in Homeland Security applications that neutron detectors shall maintain their performance in presence of gamma radiation at a dose rate of 100 $\mu\text{Sv/h}$ at the front face of the detection assembly. Obviously this gamma background shall not trigger false neutron alarms. As detailed in [13], this gamma dose rate is produced by a ^{137}Cs source delivering 7800 photons/(s cm^2) at the front face of the detector.

Two major effects have to be considered when the detector is operated in a high gamma-ray field:

- 1) The possibility of “fake” neutron events due to physical effects as the signal pile-up as well as instabilities of the front-end electronics at high rate that might produce signals with a neutron-like shape and
- 2) The tail of the gamma-ray peak towards the neutron region in the PSD spectrum.

4.1. EJ-301 scintillator

We start considering the number of false neutrons events produced by gamma-rays in the EJ-301 liquid scintillators in

increasing the gamma-ray background by using ^{137}Cs sources placed at different distances from the detector front face.

After some preliminary tests with a 400 kBq source, a first irradiation was performed by placing a 590 MBq ^{137}Cs source at 67 cm distance from the detector. At this distance the dose rate at the surface of the detector is about 100 $\mu\text{Sv/h}$ and the detector count rate was about 50 kHz. The PSD scatter plot obtained directly by using the FPGA parameters is reported in the left panel of Fig. 4. It is clear that a large number of gamma-ray events are contaminating the neutron region. To reduce the contamination effect it is necessary to operate a pile-up rejection [8]. Moreover, an improvement of the pulse shape discrimination was also obtained in [15] by using a “hybrid” technique by software processing the digitized signals.

To filter out pile-up events or look for signals that generate fake neutrons, the digitizer was operated to record the relevant part of the digitized signal in a time window of 280 ns, which corresponds to the Long Gate integration time.

On the stored data file, a filter was applied to detect the presence of pile-up looking at multiple minima in the digitized signal. In addition, event-by-event, the FPGA parameters were compared with the same parameters derived off-line from the digitized signals. The filtering action resulted in the rejection of about 2% of events labelled as pile-up but an additional 5% of the events were discarded since they did not fulfil the quality control performed offline on the FPGA parameters. This means that at this count rate some FPGA integrations (Short or Long Gates) are not correct. For example some events have the correct total energy (i.e. the Long Gate integration) but not the Short Gate integration resulting in a wrong determination of the PSD parameter.

The result of this action is shown in Fig. 4 where the distribution of accepted and rejected events after the filtering is reported. It appears that the filtering operation eliminates all spurious gamma-ray events that would end up in the wrong region of the scatter plot.

Once the event filtering strategy was established, the ^{252}Cf source was placed at 15 cm from the detector face together with the 590 MBq ^{137}Cs source to test the possibility of detecting the weak neutron source in a high gamma-ray field as required in Homeland Security applications. The obtained PSD plot of the gamma-neutron test after the filtering is reported in Fig. 5 showing that the neutron-gamma discrimination is good enough to detect the presence of the neutron source.

We then considered the problem related to the tail of the gamma-ray distribution in the neutron region. This effect is shown in Fig. 6 where one-dimensional PSD distributions are shown with the low energy threshold $E=300$ keV for different

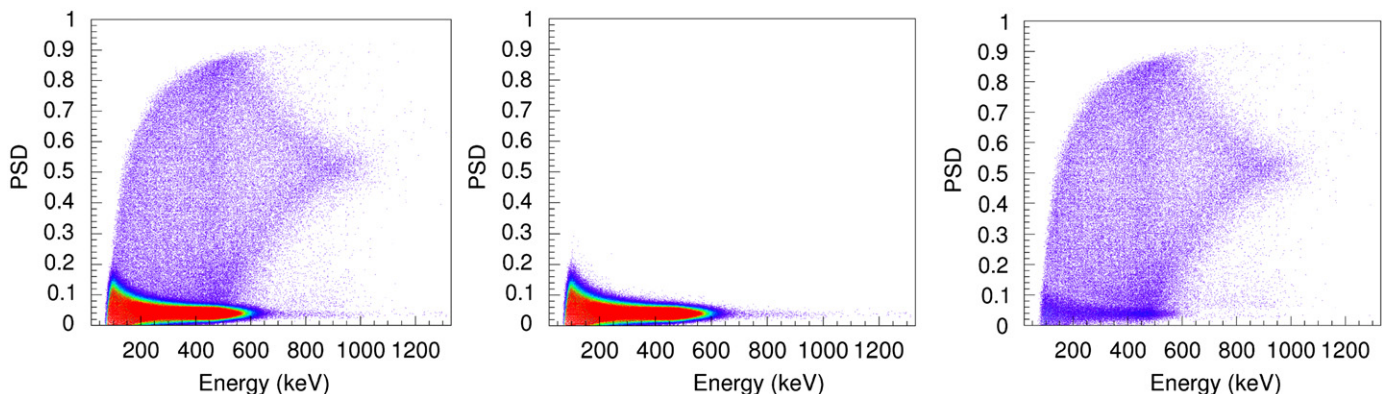


Fig. 4. PSD scatter plot from the EJ-301 scintillator irradiated with ^{137}Cs source at the dose rate of 100 $\mu\text{Sv/h}$. Left: scatter plot obtained from the FPGA processed parameters. Centre: scatter plot after the off line event filtering and Right: rejected events. Note that simply looking at the colour code might be misleading, in fact the rejected events represent only about 5% of the total. For details see the text.

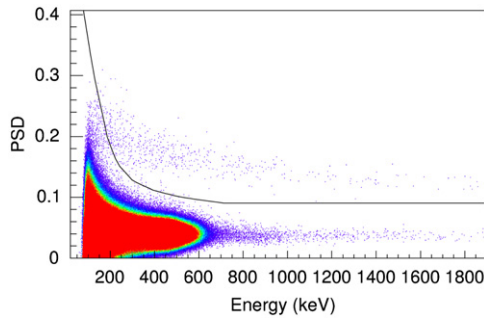


Fig. 5. PSD scatter plot after off line filtering for a weak ^{252}Cf source in the high gamma-ray background corresponding to $100\ \mu\text{Sv/h}$. For details see the text. The line shows the boundary for neutron-gamma events discrimination.

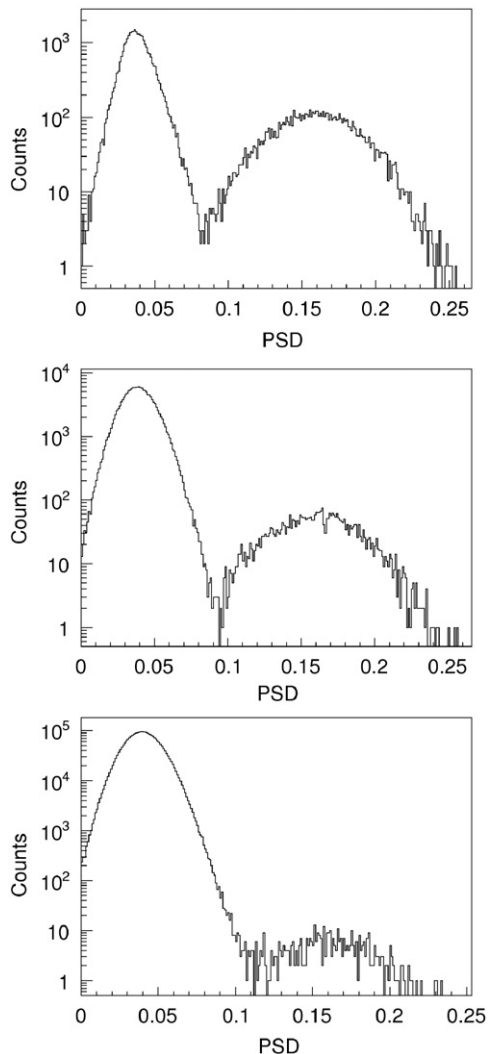


Fig. 6. Neutron-Gamma PSD distribution for a low energy threshold corresponding to 300 keV. Top: ^{252}Cf source; Middle: ^{252}Cf source in a $1\ \mu\text{Sv/h}$ gamma-ray background and Bottom: ^{252}Cf source in a $100\ \mu\text{Sv/h}$ gamma-ray background.

irradiations: ^{252}Cf source alone (top panel) ^{252}Cf and ^{137}Cs sources with the gamma-ray dose rate of $1\ \mu\text{Sv/h}$ (middle panel) and $100\ \mu\text{Sv/h}$ (bottom panel). In this representation of the data the neutrons are well discriminated from the gamma-ray even when the relative yield of the gamma-rays is increased by several order of magnitudes. It appears, however, that the PSD threshold for the neutron identification needs to be slightly increased from 0.09 to 0.11 to compensate for the spill of events from the gamma peak at

larger PSD values. This means that it is rather difficult to identify neutrons by a simple condition on the PSD parameter independent from the gamma-ray dose rate.

To optimize the neutron-gamma separation for the different gamma-ray background conditions, a polynomial function was defined, as shown in Fig. 5, to define the boundary of the neutron region in the PSD scatter plot. This separation line works good also for lower intensity gamma-ray background.

With such definition of the separation line, the effect of the event filtering and neutron events selection was studied in detail by looking at the neutron counts for different conditions:

- The laboratory room background;
- The ^{252}Cf source placed at 15 cm from the detector;
- The $100\ \mu\text{Sv/h}$ irradiation with ^{137}Cs only and
- The irradiation as in (c) but with the ^{252}Cf source as in (b).

The results in term of the average number of detected neutrons for 10 s time bins are reported in Table 1 showing the impressive effect of the software filtering: in a high intensity gamma-ray field more than 6000 “fake” neutrons counted in 10 s are rejected allowing the detection of the ^{252}Cf source. Moreover the software filter does not reject true neutron events, therefore detecting a weak neutron source in a strong gamma-ray background with an extremely good signal-to-background ratio $S/B=54/0.7=77$.

Finally, the false alarm rate (FAR) and the probability of detection (PD) was determined following the prescriptions of [16] for 10 s sampling time, as required by the standard IEC62327 for hand-held instruments [14]. Results are reported in Table 2. We started with a long room background run that provided 188 sets of data each of 10 s sampling time. The average number of detected neutrons was so low that the threshold for neutron alarm was set to $N > 1$ neutron event. With this threshold, the probability of positive false alarm was about 0.53% with the room background and about 5% with the high gamma-ray background. On the contrary, the probability of alarm with the ^{252}Cf source was 100% in both experimental configurations.

The results reported in Table 3 demonstrate that the probability of detection of the ^{252}Cf source is $PD=95\%$ at 95%

Table 1

Average neutron counts registered for 10 s time bins with the EJ-301 scintillator for different irradiations. For details see the text.

Irradiation	Neutron counts without filter	Neutron counts with filter
Background	0.1	0.1
$^{252}\text{Cf}@15\ \text{cm}$	58	56
$^{137}\text{Cs}@100\ \mu\text{Sv/h}$	6.1×10^4	0.7
$^{137}\text{Cs}@100\ \mu\text{Sv/h}$ and $^{252}\text{Cf}@15\ \text{cm}$	6.1×10^4	54

Table 2

Neutron alarms with the EJ-301 scintillator in different irradiations. For details see the text.

Irradiation	Number of trials	Number of neutron alarms
Background	188	1 (0.53%)
$^{252}\text{Cf}@15\ \text{cm}$	59	59 (100%)
$^{137}\text{Cs}@100\ \mu\text{Sv/h}$	58	3 (5%)
$^{137}\text{Cs}@100\ \mu\text{Sv/h}$ and $^{252}\text{Cf}@15\ \text{cm}$	61	61 (100%)

Table 3
Same as Table 1 but for the EJ-309 scintillator.

Irradiation	Neutron counts without filter	Neutron counts with filter
Background	1.0	0.1
$^{252}\text{Cf}@15\text{ cm}$	60	57
$^{137}\text{Cs}@100\ \mu\text{Sv/h}$	5.6×10^4	1
$^{137}\text{Cs}@100\ \mu\text{Sv/h}$ and $^{252}\text{Cf}@15\text{ cm}$	5.6×10^4	53

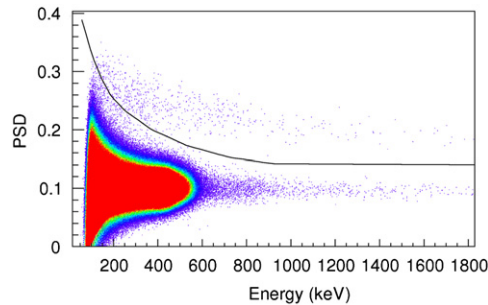


Fig. 7. Same as Fig. 5 but for the EJ-309 scintillator.

confidence level in both cases of gamma-ray background. It is also worth noting that the false alarm rate is strongly dependent on the alarm threshold $N > 1$. We recall that such low threshold was set considering the very low counting rate of neutrons in the room background. This low threshold would allow us to detect extremely low intensity neutron sources in standard natural gamma-ray background. On the other hand a slight increase of the threshold value would result in a substantial reduction of the false alarm rate in a strong gamma-ray background.

4.2. EJ-309 scintillator

The experimental tests described in Section 4.1 were repeated with the EJ-309 scintillator obtaining results very close to those of EJ-301.

The PSD scatter plot obtained after software filtering for the ^{252}Cf and ^{137}Cs at $100\ \mu\text{Sv/h}$ dose rate irradiation is reported in Fig. 7 along with the polynomial line used to discriminate gamma-ray and neutrons with EJ-309.

It appears from Fig. 7 that a sufficiently good discrimination is obtained after software filtering also using the EJ-309 scintillator. Numerical results in terms of average number of detected neutrons for 10 s time bins are reported in Table 3 showing that the behaviour of the EJ-309 scintillator is substantially the same as EJ-301: with the off line software filtering the number of “fake” neutrons is almost zeroed so that the detection of a ^{252}Cf source appears to be possible also in this case. However one should mention that EJ-309 exhibits events with an irregular signal shape giving rise to a certain number of “fake” neutrons when processed by the FPGA even at low gamma-ray intensities, typical of natural room background. Nevertheless the software filter rejects such “fake” neutrons. Finally in Table 4 we present results on false alarms and detection capability of the EJ-309 scintillator.

Also in this case the threshold for the neutron alarm is $N > 1$ event and the probability of positive false alarms is about $\text{FAR}=4.8\%$ in the high gamma-ray background. The probability of detection is $\text{PD}=95\%$ at 95% confidence level.

As a conclusion the performances of EJ-309 measured in this work are essentially equivalent to those of EJ-301.

Table 4
Same as Table 2 but for the EJ-309 scintillator.

Irradiation	Number of trials	Number of neutron alarms
Background	188	4 (2.1%)
$^{252}\text{Cf}@15\text{ cm}$	59	59 (100%)
$^{137}\text{Cs}@100\ \mu\text{Sv/h}$	62	3 (4.8%)
$^{137}\text{Cs}@100\ \mu\text{Sv/h}$ and $^{252}\text{Cf}@15\text{ cm}$	63	63 (100%)

5. Measurements at higher dose

Additional short irradiations were also performed by changing the 590 MBq ^{137}Cs source-detector distance to 47 and 37 cm, which correspond to a dose rate of 200 and 300 $\mu\text{Sv/h}$ respectively. In such conditions, it is still possible to identify neutrons after software filtering. This is shown in Fig. 8 where PSD scatter plots are reported for the EJ-301 and EJ-309 scintillators irradiated by the ^{137}Cs at 37 cm and ^{252}Cf sources with and without the software off-line filtering.

It is worth mentioning that in those irradiations the rejection of events was quite high: about 4% of the events were rejected because of the pile-up filter and 10% after the FPGA quality check. The possibility of performing PSD in such extreme conditions is also documented in Fig. 9 where the PSD distributions are shown for the two scintillators with a low energy threshold of 300 keV.

6. Summary and conclusions

The pulse shape discrimination capability of EJ-301 and EJ-309 liquid scintillation detectors by using fast digitizers has been studied in this work. The study was performed in order to verify the possibility of using novel liquid scintillation detectors without chemical and fire hazards in Homeland Security applications.

We found confirmation that the EJ-309 liquid scintillator exhibits a slightly lower PSD capability when compared to the EJ-301 characterized by high chemical toxicity and high flammability.

As for the capability of detecting weak neutron sources in a strong gamma-ray background, it is found that “fake” neutron events generated by the gamma-ray high rate may completely hide the neutron signal if only on-line processing is done. The application of an off-line software filter largely improves the situation, removing almost completely both pile-up signals and faulty parameters generated by the FPGA. When such filter is applied a weak neutron source in conditions described by the IEC62327 standard for hand-held instruments is detected with 95% probability at 95% confidence level with both types of scintillators. A positive false alarm rate of about 5% is registered when a very low threshold for neutron alarm (fixed for room background conditions) is employed. The false alarm rate could be strongly reduced by using a dynamically defined neutron threshold as a function of the gamma-ray count rate obtaining in this way the largest possible sensitivity in normal operating conditions (i.e. for low intensity gamma-ray background) and a reduction of the FAR for increasing gamma rate.

Finally, it is worth mentioning that the computing time needed for the software filter is compatible with real time operations. For 10 s sampling time, the time needed to process all data (about 0.5 Mevents) is of the order of 15 s. The computing time is reduced to 2 s when only the events in the neutron region are filtered, which represents presumably the most interesting situation for Homeland Security applications.

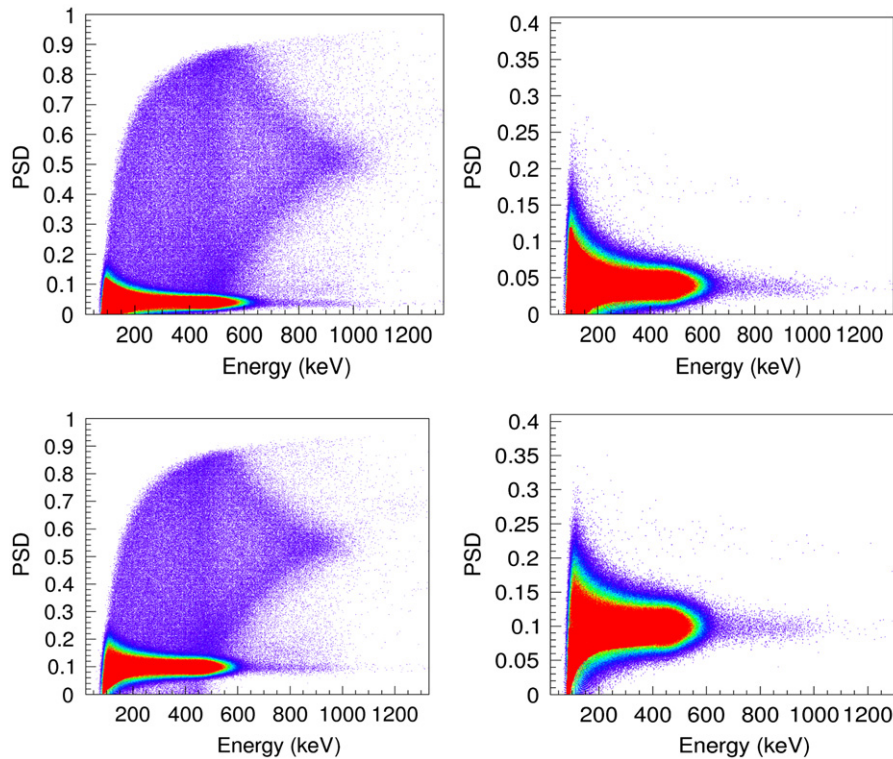


Fig. 8. PSD scatter plot before (left panel) and after off line filtering (right panel) for a weak ^{252}Cf source in the high gamma-ray background corresponding to $300\ \mu\text{Sv/h}$. Top: EJ-301. Bottom: EJ-309.

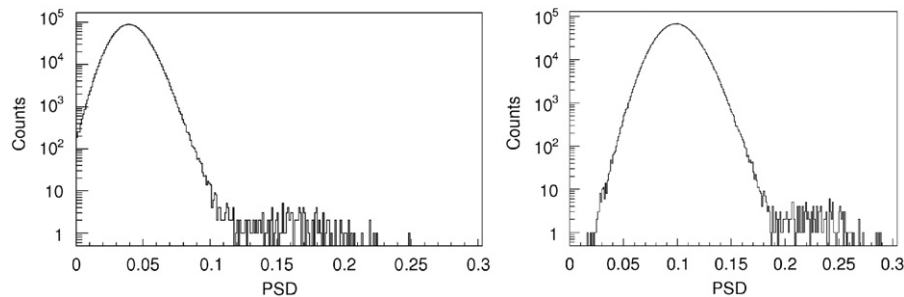


Fig. 9. PSD distribution for the EJ-301 (left panel) and EJ-309 (right panel) scintillators in case of the weak ^{252}Cf source in the high gamma-ray background (dose rate $300\ \mu\text{Sv/h}$) with a low energy threshold of 300 keV. For details see the text.

In conclusion, the preliminary measurements reported here show that the detection of neutrons is possible even at large gamma-ray dose rate. It seems that liquid scintillation detectors with modern digital read-out and opportune software filtering might be usefully employed in Homeland Security applications to detect fast neutrons. It will be interesting to test whether the same conclusions can be drawn for the novel solid scintillators that exhibit a good neutron/gamma pulse shape discrimination capability [17,18].

References

- [1] H. Klein, F.D. Brooks, in: Proceedings of the FNDA2006 Conference. Paper 097 and references therein, 2006.
- [2] F.D. Brooks, H. Klein, Nuclear Instruments and Methods in Physics Research Section A 476 (2002) 1.
- [3] R.C. Runkle, Nuclear Instruments and Methods in Physics Research Section A 652 (2011) 37.
- [4] R.T. Kouzes, et al., Nuclear Instruments and Methods in Physics Research Section A 587 (2008) 89.
- [5] see <http://www.eljentechnology.com/images/stories/Data_Sheets/Liquid_Scintillators/EJ-309%20data%20sheet.pdf>.
- [6] S.A. Pozzi, S.D. Clarke, M. Flaska, P. Peerani, Nuclear Instruments and Methods in Physics Research Section A 608 (2009) 310.
- [7] A. Lavietes, et al., in: Proceedings of the International Safeguards Symposium 2010, Vienna, November 2010, <<http://www.iaea.org/OurWork/SV/Safeguards/Symposium/2010/Documents/PapersRepository/340.pdf>>.
- [8] L. Swiderski, et al., Nuclear Instruments and Methods in Physics Research Section A 652 (2011) 330.
- [9] J.R.M. Annand, Nuclear Instruments and Methods in Physics Research Section A 262 (1987) 371.
- [10] L. Stevanato, et al., Applied Radiation and Isotopes 69 (2011) 369.
- [11] N.V. Kornilov, I. Fabry, S. Oberstedt, F.-J. Hamsch, Nuclear Instruments and Methods in Physics Research Section A 599 (2009) 226.
- [12] J. Iwanowska, et al., Journal of Instrumentation (JINST) 6 (2011) P07007.
- [13] R.T. Kouzes, et al., Nuclear Instruments and Methods in Physics Research Section A 654 (2011) 412.
- [14] M. Voytchev, P. Chiaro, R. Radev, Radiation Measurements 44 (2009) 1.
- [15] S.D. Ambers, et al., Nuclear Instruments and Methods in Physics Research Section A 638 (2011) 116.
- [16] D. Gilliam, et al., Journal of Research of the National Institute of Standards and Technology 114 (2009) 195.
- [17] C. Matei, F.-J. Hamsch, S. Oberstedt, Nuclear Instruments and Methods in Physics Research Section A 676 (2012) 135–139.
- [18] N. Zaitseva, et al., Nuclear Instruments and Methods in Physics Research Section A 668 (2012) 88.